CHAPTER 3

BOUNDARY LAYER DYNAMISM AND PM2.5-PBLH INTERACTION OVER BRAHMAPUTRA VALLEY AT THE VALLEY-SITE SCALE

3.1 INTRODUCTION

In the previous chapter, the interaction and spatio-temporal variation in PM2.5, AOD 550 nm and meteorological parameters are studied. The concentrations of aerosols are also highly influenced by a change in PBLH. The spatial and diurnal analysis of PBLH and PM2.5, and PM2.5-PBLH relationship over the complex terrain of BV using data from MERRA-2, ERA5 ECMWF and GPS radiosonde forms the core of investigation in this chapter.

The planetary boundary layer (PBL), the lowest part of the atmosphere, has a profound influence on the atmospheric process, climate system and air quality. It acts as a turbulent buffer (that regulates the exchange of heat, momentum, moisture, dust and aerosols) between the earth's surface and the free atmosphere [1-4]. The exchange of aerosols through the PBL is mostly controlled by the atmospheric processes such as convective turbulence and advection (dispersion, transport, transformation and deposition) [1, 5]. These atmospheric processes in the PBL directly respond to terrain-induced flow modification, heat flux, frictional drag and pollutant emission which are apparent over a complex terrain [1, 2, 6]. Complex terrain not only exerts an important influence on boundary layer flow [6] but also affects the atmospheric transport and mixing of aerosols at a broad range of spatial and temporal scales [7-9]. The vertical scale of this transport and mixing of aerosol with the free atmosphere is determined by PBLH, one of the most relevant boundary layer properties to investigate PBL [9, 10].

PBLH is a fundamental parameter that characterizes the vertical mixing between the earth's surface and free atmosphere through the PBL [3, 4]. The convective and turbulent processes that control vertical mixing within PBLH are complex and vary on a wide range of parameters like space, time scales and terrain. PBLH variability is driven by multiple forcing mechanisms including the diurnal and seasonal cycle of incoming solar radiation, advection, turbulence, synoptic-scale subsidence, and terrain-induced flow modification [1-2, 11-12].

The concentrations of aerosols are highly responsive to changes in PBLH; during day-time high PBLH (convective boundary layers CBL) generated by the convective updrafts, increases vertical diffusion of aerosols and reduces their concentrations. While during night-time low PBLH (shallow stable boundary layer SBL), reduces vertical diffusion of aerosols, and therefore, increases aerosol concentration [13, 14]. In addition, the

accumulation, dispersion, and fate of aerosol are also dictated by several chemical, physical and dynamic atmospheric processes that are relevant to PBL [5, 11, 15, 16 and the reference therein].

As mentioned earlier, BV is surrounded by mountains and hills in the north, south and east (southeast), and opens towards the Indo-Gangetic Plains (IGP) in the west. The complex terrain of the valley has a cumulative effect on the diurnal and seasonal evolution of PBLH, which in turn plays a significant role in the accumulation of local and long-range transported aerosol and its residence [17]. In addition, the biogenic, carbonaceous and marine sea salt aerosols from the huge forest cover, open burning of solid waste disposal [18] and the Bay of Bengal contribute to aerosols loading over the valley [17, 19-21]. The meteorological conditions associated with the Asian summer monsoon over the Indian subcontinent [22] are implicit in ensuring a typical role in boundary layer dynamics and aerosol environment over the region. Diurnal variability of PBLH is one of the prime factors in the variation of surface PM2.5, PM10, and black carbon (BC) over the BV [21, 23]. PBLH, in turn, is a function of turbulent mixing, horizontal high wind speeds, fumigation effect and subsidence in PBL over BV [17, 20, 24-26].

The high pollutant load of the IGP enters the BV from the west [21]. Consequently, PM2.5 concentrations in the largest city, Guwahati, of BV are about five-fold higher than the USEPA standards [17]. The unique topography of the valley, atmospheric processes modified by terrain complexity, boundary layer dynamic, abundance of local sources (particularly biogenic aerosols), entrapment of long-range transported aerosols in the PBL, and the extant state of air quality, make the valley significant to aerosol-PBLH studies. Despite its importance, comprehensive investigation of diurnal changes in PM2.5 and PBLH and the association is virtually non-existent at the valley-site scale.

This study, therefore, investigates (a) the variability of PBLH and surface PM2.5 concentration at the spatial and diurnal scale; (b) seasonality of PBLH, PM2.5 and AOD 550 nm; and (c) the association of PBLH with surface PM2.5 concentration in different seasons over BV. All these investigations are carried out at the valley-site scale. To the best of the author's knowledge, this study is the first to report the diurnal and seasonal variability of PBLH, and the PM2.5-PBLH relationship at the valley-site scale for BV.

In addition, this study also attempts to overcome the limitations of inadequate ground-based data at a high spatial and temporal scales for PBLH and PM2.5; a longstanding and major limitation of aerosol-PBLH research over the valley. The data limitations can be effectively overcome by the use of satellite-derived aerosol products and reanalysis data. This study utilizes MODIS onboard Terra and Aqua AOD retrievals, ERA5 reanalysis and MERRA-2 PBLH data, and surface GPS radiosonde PBLH estimates.

3.2 DATA, SOURCES AND PRE-PROCESSING

The details of the datasets along with sources used in this study are provided in Table 3.1 and the salient features are discussed in the following sub-sections. The ground-based GPS radiosonde data station is shown in Figure 3.1.

Table 3.1 Technical specifications of the datasets used.

Parameters	Spatial resolution	Temporal resolution	Data source	Available at
BLH	0.25º x 0.25º	hourly	ERA5 ECMWF	https://www.ecmwf.int/en/forecasts/datasets/browse-reanalysis-datasets
PBLH	0.5º x 0.625º	hourly	MERRA-2	https://gmao.gsfc.nasa.gov/reanalysis/MERRA-2/
Temperature, pressure, RH, θ, θ_V, WS and WD	point	00:00 h UTC and 12:00 h UTC	GPS radiosonde	http://weather.uwyo.edu/upperair/sounding.html
Aerosol components: BC, SO_4, $SS_{2.5}$, $DU_{2.5}$, OC	0.5º x 0.625º	hourly	MERRA-2	https://disc.gsfc.nasa.gov/
AOD 550 nm	10 x 10 km	10:30 LST and 13:30 LST	MODIS Terra and Aqua	https://ladsweb.modaps.eosdis.nasa.gov/search/

θ= potential temperature; θ_V= virtual potential temperature, WS= wind speed, WD= wind direction, BC= Black carbon, SO_4= sulfate, $SS_{2.5}$= sea salt, $DU_{2.5}$= dust, OC= organic carbon

3.2.1 ERA5 ECMWF BLH

ERA5 ECMWF reanalysis hourly estimates of boundary layer height (BLH) were downloaded and extracted at 0.25^0 x 0.25^0 native spatial resolution for the study period 2016-2020. ERA5 is the fifth-generation global reanalysis product by ECMWF. ERA5

BLH calculation is based on the bulk Richardson number (Ri). BLH is defined as the lowest level at which the bulk Ri reaches the critical value of 0.25 (where the surface frictional effects are ignored in the computation of the bulk shear due to lack of friction velocity from radiosonde data).

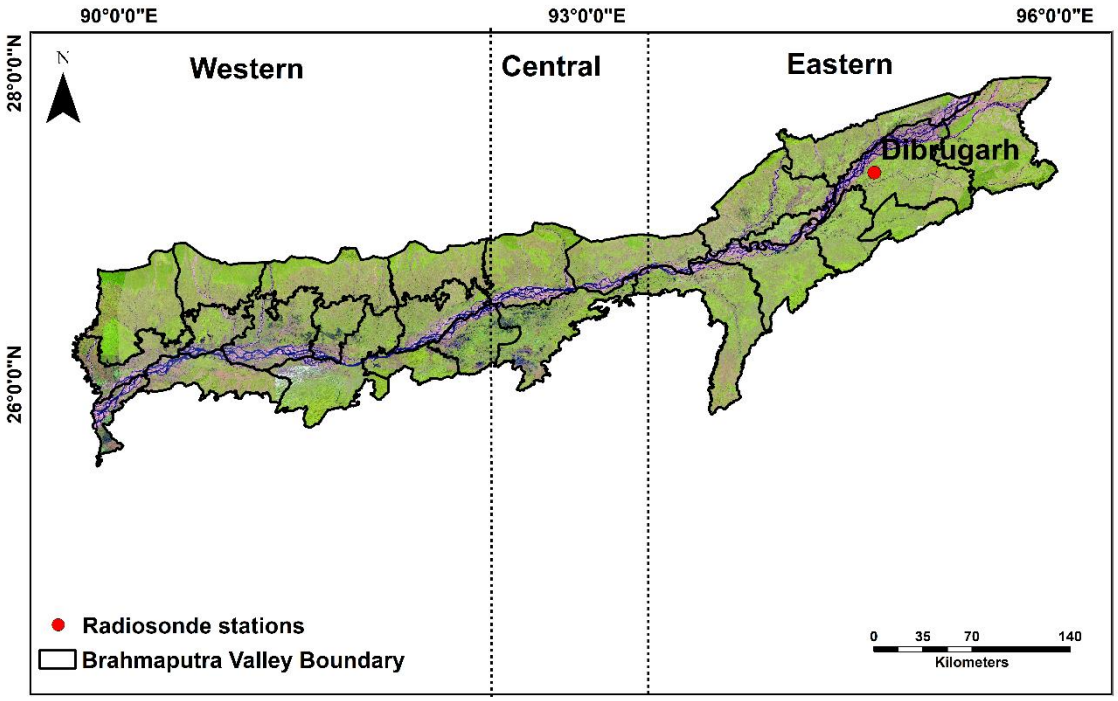

Figure 3.1 Ground-based station of GPS radiosonde, Dibrugarh.

3.2.2 MERRA-2 PBLH

MERRA-2 PBLH hourly time-averaged 2-dimensional data were acquired at 0.5° x 0.625° native spatial resolution for the study period. This global atmospheric reanalysis was produced by NASA Global Modelling and Assimilation Office (GMAO) using the Goddard Earth Observing System Model (GEOS) version 5.12.4. MERRA-2 PBLH (variable name PBLH) is calculated based on the total eddy diffusion coefficient of heat (K_h) with a threshold equal to 10% of the column maximum [27]. PBLH data is an assimilation of modern hyperspectral radiance and microwave observations along with GPS-Radio Occultation datasets and meteorological assimilation (https://gmao.gsfc.nasa.gov/reanalysis/MERRA-2/).

3.2.3 Radiosonde

GPS-based Radio-sounding system data of upper-air sounding for Dibrugarh station was collected from the Department of Atmospheric Science, University of Wyoming and used for estimation of PBLH. The sounding data are mostly available at the 00:00 h UTC (5:30 h LST) and 12:00 h UTC (17:30 h LST) time scale on daily basis. All estimates of PBLH were done for 00:00 h UTC (5:30 h LST) sounding hours with reference to the height above ground level. The estimated PBLH was used for validation of MERRA-2 and ERA5 reanalysis derived PBLH data for the Dibrugarh station.

3.2.4 MODIS AOD 550 nm

As discussed in section 2.2.1 Chapter 2.

3.2.5 PM2.5 surface concentration

As discussed in section 2.2.2 Chapter 2.

3.2.6 Data pre-processing

Collocation of data

For comparison of MERRA-2 PBLH and ERA5 BLH data with reference to radiosonde PBLH estimates, both MERRA-2 PBLH and ERA5 BLH data were extracted at their native spatial resolution 0.5^0 x 0.625^0 and 0.25^0 x 0.25^0 respectively. The reanalysis derived PBLH data were collocated in space (geo-referenced taking coordinates of Dibrugarh as the centroid) and time (00:00 h UTC) with reference to radiosonde data. The spatio-temporal collocation of the data was carried out using Python libraries.

Data integration

MERRA-2 PBLH estimates, MODIS AOD 550 nm retrievals and total PM2.5 surface concentration (generated from MERRA-2 aerosol components) were re-gridded from native spatial resolution to new target grid size 0.25^0 x 0.25^0 by using python libraries and IDW (Inverse distance weighting) method on ArcGIS10.5 and interface for BV, for 2016-2020. To examine the diurnal variation of PBLH and the concurrent surface PM2.5 concentration over the BV, the day-time and night-time mean were used. For seasonality analysis, the seasonal mean of PBLH and (concurrent) PM2.5 and AOD 550 nm was used.

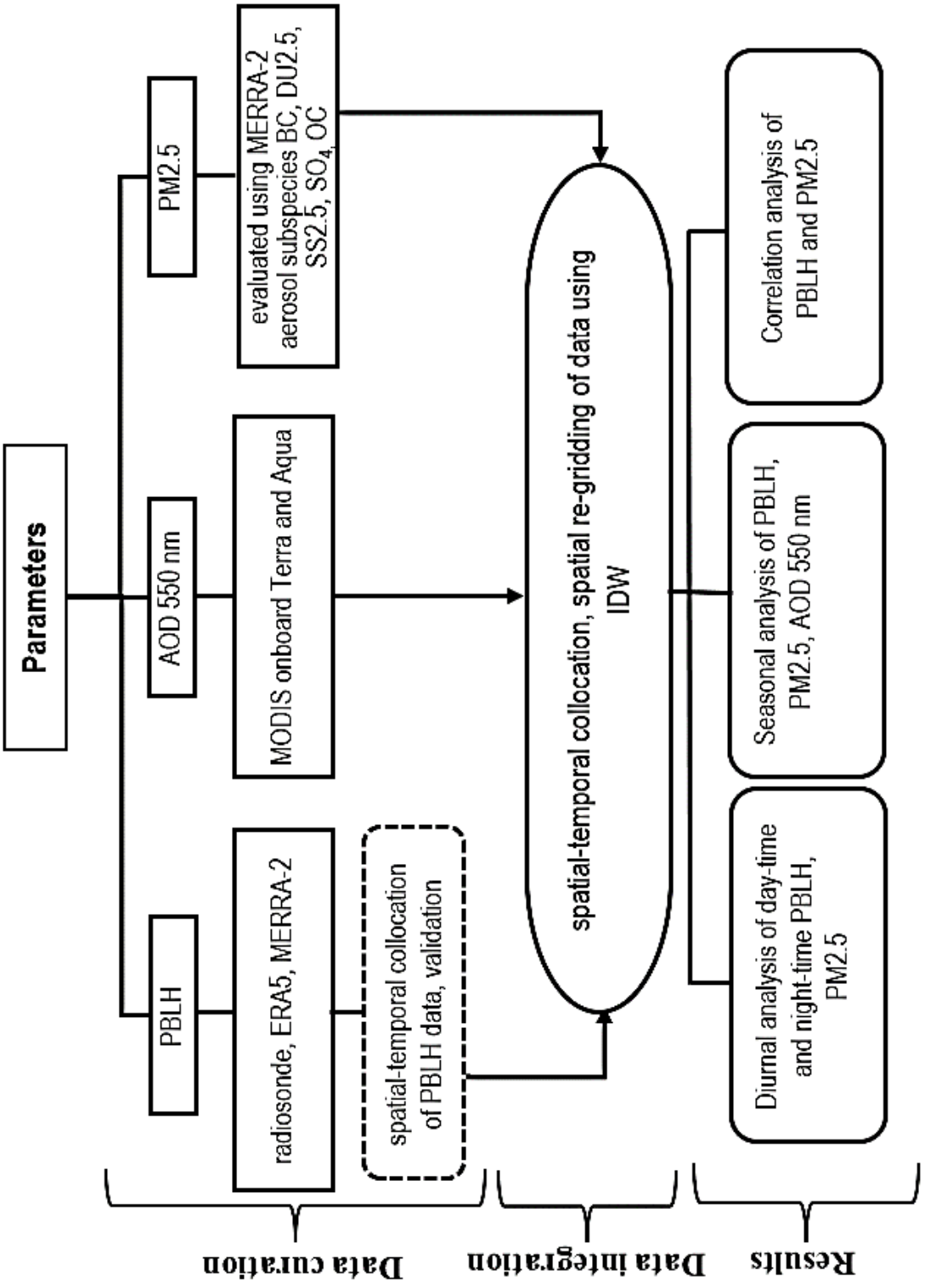

Figure 3.2 Schema of the methodology.

3.3 METHODOLOGY

The schema of the methodology used is illustrated in Figure 3.2 and the details are discussed in the following sub-sections.

3.3.1 Determination of PBLH

This study investigated the vertical gradient of 8 fundamental atmospheric fields to examine the best indicator of PBLH, over the Dibrugarh station during the early morning hours (00:00 h UTC or 05:30 h LST), 2016 (Figure 3.3a, b). The following 8 vertical gradient-based methods on profiles were examined: (1) maximum height of wind speed, (2) gradient of wind direction, (3) minimum gradient of relative humidity (RH), (4) minimum gradient of specific humidity (q), (5) maximum gradient of temperature (ºC), (6) maximum gradient of potential temperature (θ), (7) maximum gradient of virtual potential temperature (θ_v), (8) minimum gradient of refractivity (N). Out of all the vertical gradient profiles (Figure 3.3b) generated, wind speed maximum showed the sharpest gradient in the early morning hours (Figure 3.3a). The height of maximum in wind speed profile provides a good measure of mixing height during conditions of atmospheric stability over the site. PBLH, therefore, was determined from the vertical height of the maximum low-level wind speed for 2016-2019.

The atmosphere is considered stable during early morning hours (00:00 h UTC or 5:30 h LST) due to the effect of local topography. For the height of the stably stratified atmospheric boundary layer, characteristic heights of PBLH can be identified from the observed vertical profile of wind velocity [28]. The height of the maximum wind speed vertical gradient provides a good measure of mixing height during the early morning hours, as it is generally well defined from the night-time wind profiles (residual layer) [29] over the land.

Evaluation of PBLH using the Richardson number method was also attempted. However, the lack of wind data (vertical profile) at the same levels as that of the potential temperature and humidity data has led to unreliable results, therefore not included.

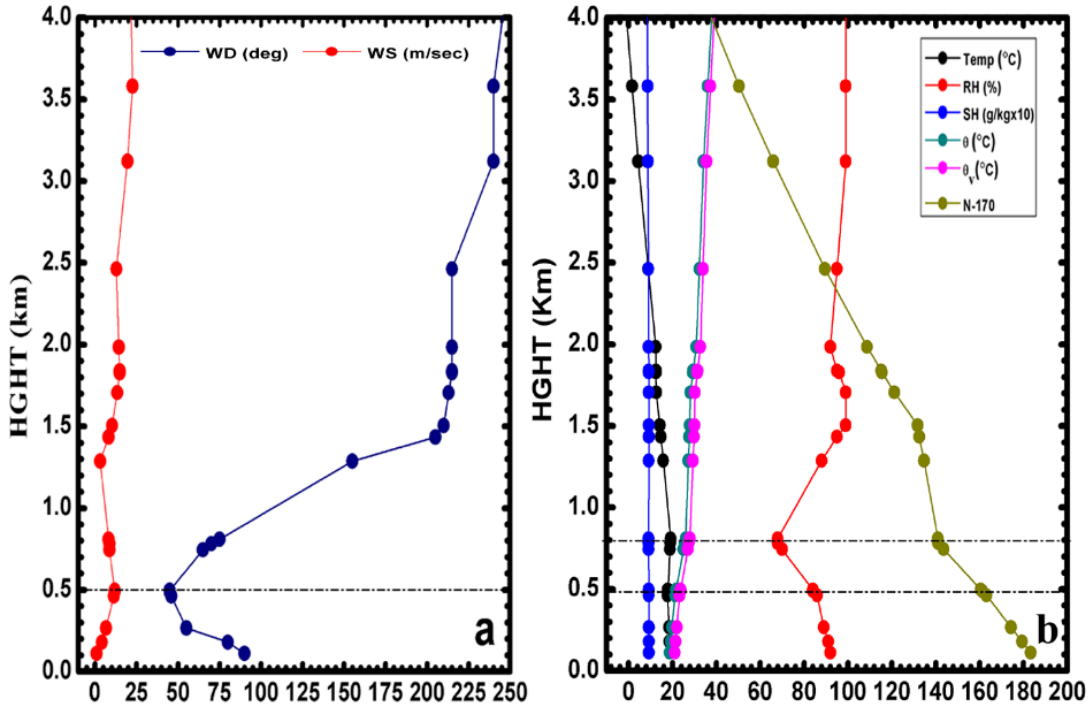

Figure 3.3 Planetary boundary layer height estimates for Dibrugarh station for 00:00 UTC 6 November 2018 using the vertical gradient-based method for eight meteorological parameters. (a) shows vertical profiles of maximum wind speed level and sharp vertical gradient of wind direction, (b) shows vertical profiles of Temperature (Temp ˚C), potential temperature (θ), virtual potential temperature (θv), relative humidity (RH %), specific humidity (SH g/kg x10), and refractivity (N)*. Estimated PBL heights are shown by dashed horizontal lines. *Some values of N are shifted for clarity.

3.3.2 Validation of PBLH data

For comparison of MERRA-2 PBLH and ERA5 BLH data with reference to radiosonde PBLH estimates, both MERRA-2 PBLH and ERA5 BLH data were extracted at their native spatial resolution 0.5^0 x 0.625^0 and 0.25^0 x 0.25^0 respectively. The reanalysis derived PBLH data were collocated in space (geo-referenced taking coordinates of Dibrugarh as the centroid) and time (00:00 h UTC) with reference to radiosonde data.

ERA5 ECMWF and MERRA-2 derived PBLH was validated with reference to radiosonde PBLH estimates for the Dibrugarh station, for the period 2016 to 2019. This was done based on statistical parameters- coefficient of determination (R^2), root mean square error (RMSE), slope and y-intercept (Figure 3.4) (details in section 4.1). MERRA-2 hourly PBLH data were extracted for day-time (10:30 h LST to 01:30 h LST) and night-

time (20:00 h LST to 23:00 h LST) in native spatial resolution, and averaged for diurnal analysis. For seasonal analysis, the mean for different seasons- winter (Jan-Feb), pre-monsoon (Mar-April-May), monsoon (Jun-Jul-Aug-Sept), and post-monsoon (Oct-Nov-Dec) were calculated using monthly PBLH data.

3.3.3 Calculation of day-time and night-time PM2.5 surface concentration

Day-time and night-time PM2.5 surface concentration was calculated for BV using hourly data of all the individual major aerosol components BC, $DU_{2.5}$, $SS_{2.5}$, OC and SO_4 employing equation (1), for the period 2016-2020. For diurnal analysis, PM2.5 surface concentration of day-time (10:30 h LST to 01:30 h LST or 05:00 h UTC to 08:00 h UTC) and night-time (20:00 h LST to 23:00 h LST or 14:30 h UTC to 17:30 h UTC) was calculated and averaged. The monthly mean of PM2.5 surface concentration was calculated using the monthly mean of all the individual aerosol components using equation (1) (below) given by Hand et al. (2011) [30]. The calculated monthly mean of PM2.5 surface concentration was averaged for each of the seasons.

$$PM2.5 = 1.375 \text{ x } [SO4] + 1.8 \text{ x } [OC] + [BC] + [DU2.5] + [SS2.5] \quad (1)$$

3.4 RESULTS AND DISCUSSION

3.4.1 Performance of ERA5 and MERRA-2 PBLH with reference to radiosonde derived PBLH

The results of performance assessment of MERRA-2 and ERA5 PBLH with respect to radiosonde PBLH estimates showed that MERRA-2 PBLH had better (R^2 = 0.482; RMSE = 1.082) represented radiosonde PBLH estimates than that of ERA5 ECMWF (R^2 = 0.0024; RMSE = 57.25) for the Dibrugarh station (Figure 3.4). MERRA-2 model PBLH is generated based on the total eddy diffusion coefficient of heat (K_h) [27] that represents the turbulent diffusion process; whereas ERA5 BLH is computed based on the bulk Richardson number method that measures local turbulence, and is often unable to properly characterize the turbulent properties of convective boundary layers (stratocumulus, shallow cumulus, and dry convective PBLs) [31]. Since the PBLH estimated in this study was from the vertical gradient of maximum wind speed, PBLH provided by the MERRA-2 dataset had a good agreement with radiosonde estimates. The

performance of MERRA-2 data (r= 0.8) is also in line with the finding of Pathak et al. (2019) [32] for the Dibrugarh station.

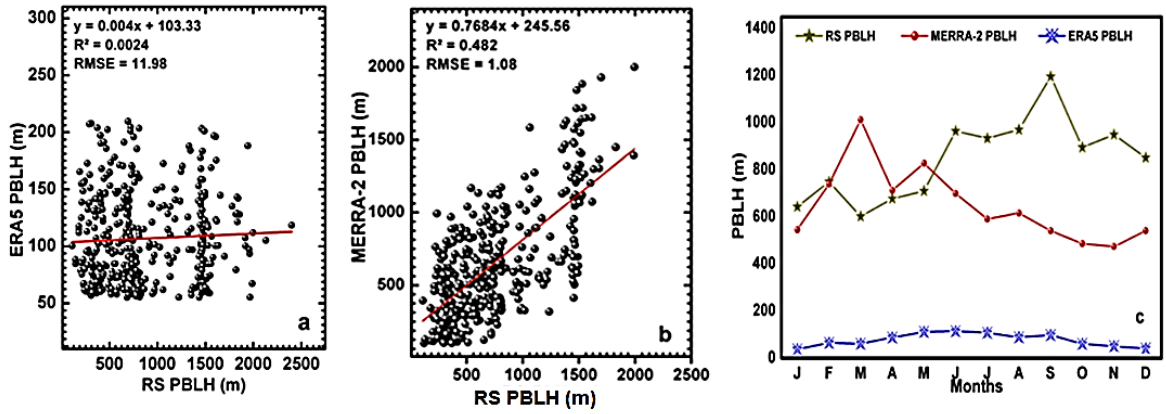

Figure 3.4 Performance assessment of (a) ERA5 PBLH and MERRA-2 (b) derived PBLH with reference to radiosonde (RS) PBLH estimates of Dibrugarh station at 00:00 h UTC (05:30 h LST), 2016-2019. (c) Comparative analysis of monthly mean of MERRA-2 and ERA5 derived PBLH, and radiosonde PBLH estimates.

3.4.2 Spatial variation of day-time and night-time PBLH and PM2.5 over BV

High spatial heterogeneity in the diurnal cycle of PBLH structure and PM2.5 across the valley was observed across seasons. PBLH observed over BV was dominated by strong diurnal variability (Figure 3.5a-d and Figure 3.6i-l) for all the seasons. PBLH was typically shallow (500 m) in evening hours (Figure 3.6i- l), when the surface layer is stable (stable boundary layer) due to infrared radiative cooling. It grows deep (to a couple of kilometres) in the afternoon hours (Figure 3.5a-d) when solar heating causes convective unstable conditions (convective boundary layer). PBLH during nocturnal periods was low, unlike day-hours; attributed to stable conditions with nocturnal inversion- a normal phenomenon over a complex terrain [11].

The deepest day-time PBLH was observed during pre-monsoon (1600-2100 m) closely followed by winter (1400-1900 m), post-monsoon (1200-1470 m) and monsoon (1190-1340 m) over the BV (Figure 3.5a-d). For night-time, shallow PBLH predominates in winter (328-931m) followed by post-monsoon (353-632 m), monsoon (355-607 m), and pre-monsoon (601-1233) m (Figure 3.6i-l).

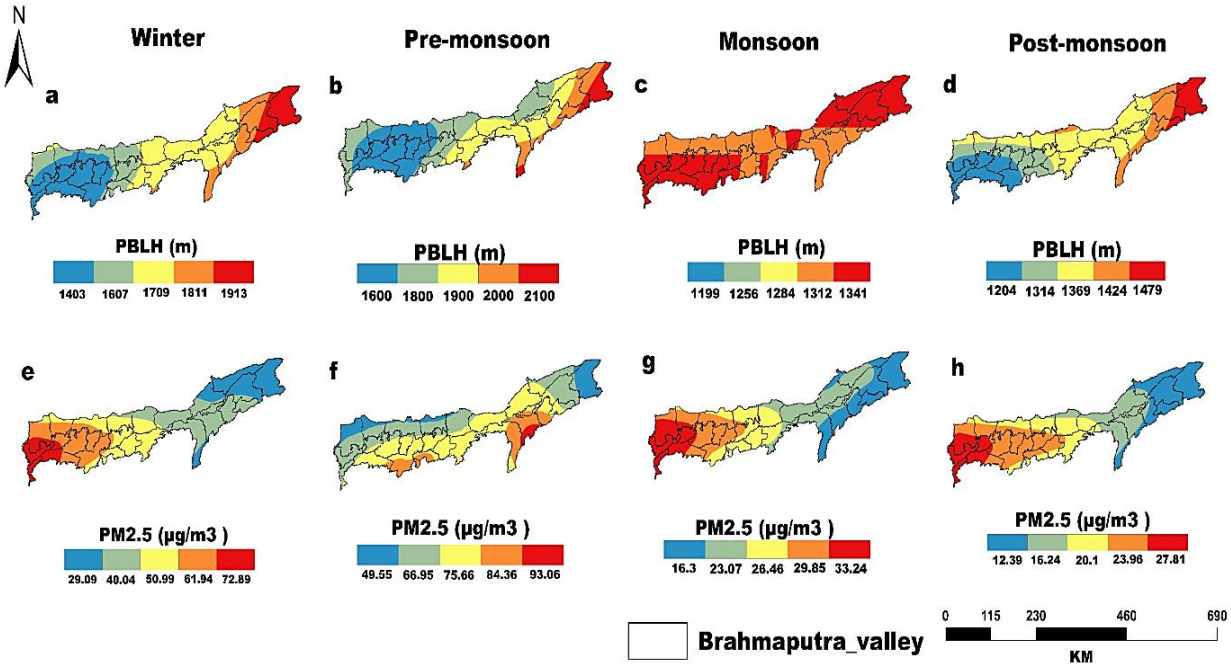

Figure 3.5 Spatial variation of (a-d) day-time (10:00 h to 13:00 h LST) mean of PBLH and (e-h) PM2.5 µg/m^3 surface concentration over Brahmaputra valley in different seasons, 2016-2020.

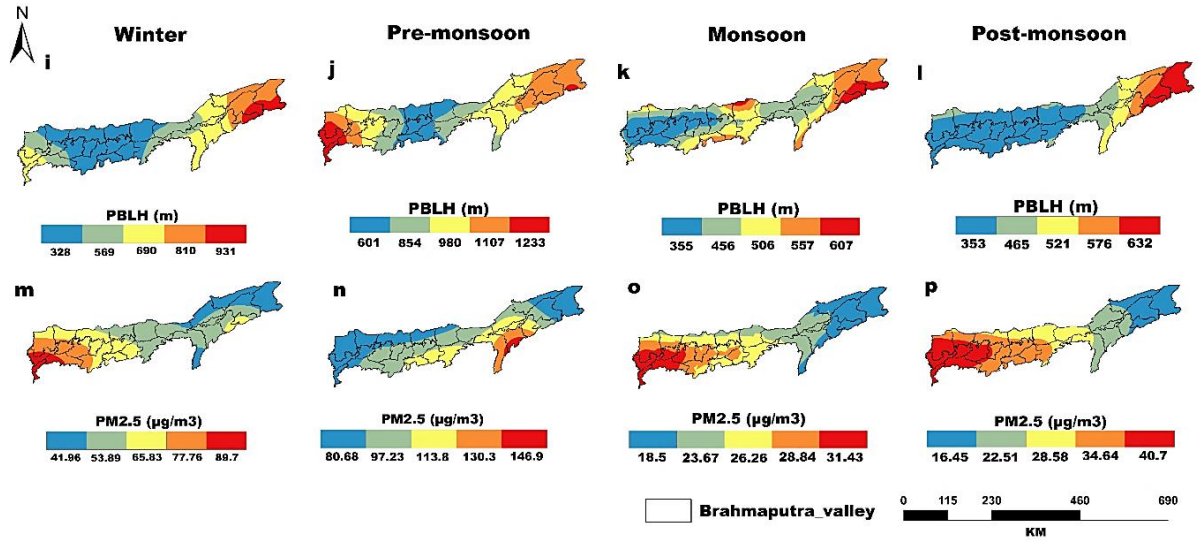

Figure 3.6 Spatial variation of (i-l) night-time (20:00 to 23:00 h LST) mean of PBLH and (m-p) PM2.5 µg/m^3 surface concentration over Brahmaputra valley across the seasons, 2016- 2020.

For PM2.5, a large diurnal variation in PM2.5 concentration was noted over BV (Figure 3.5e-h and Figure 3.6m-p). Higher PM2.5 surface concentration was observed at night-time than in the day-time. During day-time PM2.5 concentration was found to be highest in pre-monsoon (49.55- 93.06 µg/m3), followed by winter (29.09-33.24 µg/m3), monsoon (16.3-33.24 µg/m3) and post-monsoon (12.39-27.81 µg/m3) (Figure 3.5e-h). While for night-time, the highest PM2.5 concentration was noted for pre-monsoon (80.68- 146.90 µg/m3) followed by winter (41.96- 89.70 µg/m3), post-monsoon (16.45-40.70 µg/m3) and monsoon (18.5-31.43 µg/m3) (Figure 3.6m-p).

3.4.3 Synergism in PM2.5 and PBLH diurnal variability

Diurnal variation in PM2.5 concentration in the surface layer was in synergy with the diurnal cycle of PBLH over the BV (Figure 3.7a-d and Table 3.2). The pronounced diurnal evolution of PBLH and PM2.5 over the valley, reveals that turbulent mixing of air (mechanical turbulence generated by wind shear) plays, understandably, a dominant role in the entrainment of aerosols in PBL. Day-time PBLH (Figure 3.7a) was much higher than that of night-time (Figure 3.7b), while PM2.5 concentration displays the reverse trend of being much lower during day-time (Figure 3.7a) than at night-time (Figure 3.7b). Lower day-time PM2.5 concentration was possibly the outcome of vertical mixing caused by thermal and mechanical turbulence within the PBLH. The diurnal heating and cooling of hill slopes often develop thermal turbulence over complex topography [11]. It enables lifting dust and other aerosol particles from the surface and spreading them throughout the entrainment zone of PBLH. During the night, nocturnal radiative cooling of the surface leads to the formation of a ground-based stable inversion layer (nocturnal inversion), that confines aerosol mixing to a shallow layer near the surface, increasing their surface concentration.

PBLH generally becomes shallower under the influence of large-scale subsidence (downward motion), which can weaken the vertical mixing of aerosols and increase surface accumulation [33] over the area.

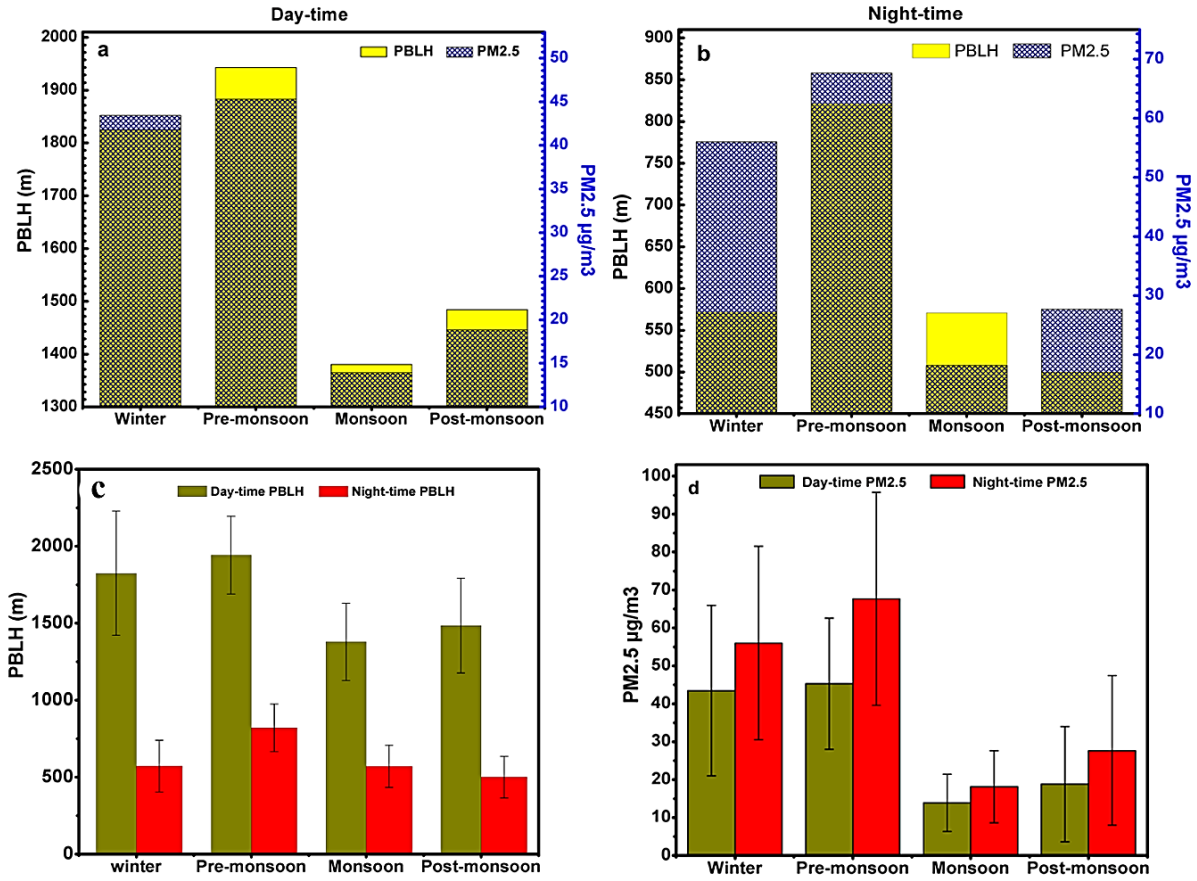

Figure 3.7 Comparative analysis of the (valley-site scale) mean (a) day-time PBLH vs day-time PM2.5, (b) night-time PBLH vs night-time PM2.5, (c) day-time vs night-time PBLH, (d) day-time vs night-time PM2.5 across the seasons, Brahmaputra valley, 2016-2020. Vertical error bar represents the standard deviation in dataset.

Table 3.2 Descriptive statistics of daytime and night-time PBLH and PM2.5 in different seasons, Brahmaputra valley, 2016-2020.

Seasons	Statistics	Day-time PM2.5 (µg/m3)	PBLH (m)	Night-time PM2.5 (µg/m3)	PBLH (m)
Winter	**Mean**	50.38	1580.37	62.83	510.35
	Min	30.70	1238.91	32.70	321.11
	Max	77.56	1865.24	93.70	827.03
	Median	46.94	1579.30	61.95	506.60
	SD	12.09	167.68	14.68	151.12
Pre-monsoon	**Mean**	49.81	1797.21	70.42	866.34
	Min	40.84	1491.89	51.02	586.44
	Max	57.18	2060.13	101.98	1234.06
	Median	51.71	1765.11	68.83	851.85
	SD	4.72	148.43	12.58	163.63
Monsoon	**Mean**	16.20	1219.39	21.14	478.27
	Min	11.50	1007.97	13.66	372.64
	Max	23.54	1498.15	31.66	629.59
	Median	15.44	1221.27	19.74	472.21
	SD	3.48	139.10	5.47	77.71
Post monsoon	**Mean**	20.32	1292.27	30.36	422.44
	Min	8.92	1043.23	11.29	259.90
	Max	43.38	1535.25	59.77	702.46
	Median	17.99	1297.91	27.54	409.17
	SD	8.54	133.17	11.85	97.78

PBLH= Planetary boundary layer height

3.4.4 Seasonal changes of PM2.5, AOD 550 nm and PBLH over BV

The climatology of the PBLH, especially its seasonal variability, is important for air pollution related studies. PBLH derived from MERRA-2 was utilised to represent the seasonality of PBLH across the spatial domain of BV. The seasonal mean of PBLH, AOD 550 nm and surface PM2.5 concentration of the entire BV are represented in Figure 3.8. PBLH was observed higher in pre-monsoon closely followed by winter, post-monsoon and monsoon. PBLH was the deepest in pre-monsoon (939.40 to 1414.07 m), and the shallowest in monsoon (487.57- 817.92) over the BV (Figure 3.8a-d).

For all the seasons, PM2.5 surface concentration and AOD 550 nm displayed high spatial variability similar to PBLH variation. This pattern is in conformity with observations from other research work [34-35]. Relatively larger amounts of PBLH with lower levels of PM2.5 (Figure 3.8e-h) and AOD 550 nm (Figure 3.8i-l) prevailed over the eastern

parts of BV, compared to the western and central. Deeper PBLH over the eastern BV could be due to the higher turbulence developed over the rough landscape (of the eastern BV), relative to the turbulence developed in the other parts. The eastern part of BV, which comprises hill ranges, dense vegetation cover and vast floodplains, is suitable for developing strong mechanical and convective turbulence (eddy motion). The results indicate that turbulence within the PBLH is effective in regulating the PM2.5 surface concentration across the entire valley.

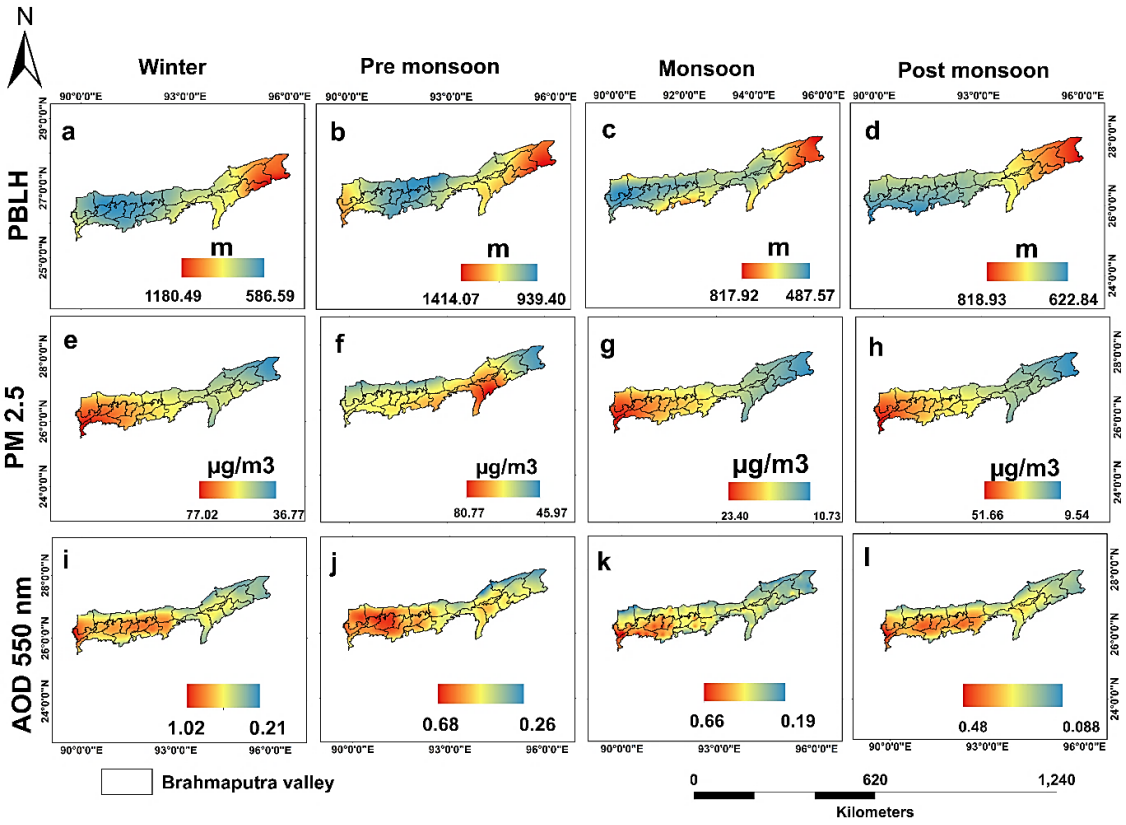

Figure 3.8 Variation in seasonal mean of (a-d) PBLH, (e-h) PM2.5 concentration and (i-l) AOD 550 nm over Brahmaputra valley, 2016-2020.

3.4.5 PBLH-PM2.5 relationship

Positive association between PBLH and PM2.5 was observed for all the seasons (Figure 3.9a-d). In winter, the eastern parts of BV showed relatively stronger positive relation (r= 0.66 to 0.91; $0.0001 \leq p \leq 0.17$), than the central (r= 0.34 to 0.66; $0.17 \leq p \leq 0.33$) and western parts (r= 0.02 to 0.46; $0.33 \leq p \leq 0.95$) (Figure 3.9a and Figure 3.10a). During pre-monsoon, most areas in the central and western parts of the valley showed weak to moderate positive relation (r= 0.172 to 0.59, $0.02 \leq p \leq 0.22$), whereas eastern parts showed strong positive relationship (r= 0.59 to 0.66; $0.007 \leq p \leq 0.02$) (Figure 3.9b and Figure 3.10b). In the monsoon, weak (r= 0.04 to 0.32; $0.08 \leq p \leq 0.86$) to moderate (r= 0.40 to 0.59; $0.006 \leq p \leq 0.008$) relationship predominated over the valley (Figure 3.9c and Figure 3.10c). Whereas, poor to strong PBLH-PM2.5 relationship (r= 0.007 to 0.59; $0.02 \leq p \leq 0.98$) prevailed in the post-monsoon season (Figure 3.9d and Figure 3.10d). The eastern BV represented unusual strong positive PBLH-PM2.5 relationship consistently for the three consecutive seasons: winter, pre-monsoon and monsoon. Eastern BV is less polluted and represents the highly heterogeneous terrain, and forested landscape as compared to the western and central parts. Low p-value [≤ 0.05 correlation significant at the 0.05 level (2-tailed)] suggests that changes in the PM2.5are associated with changes in PBLH.

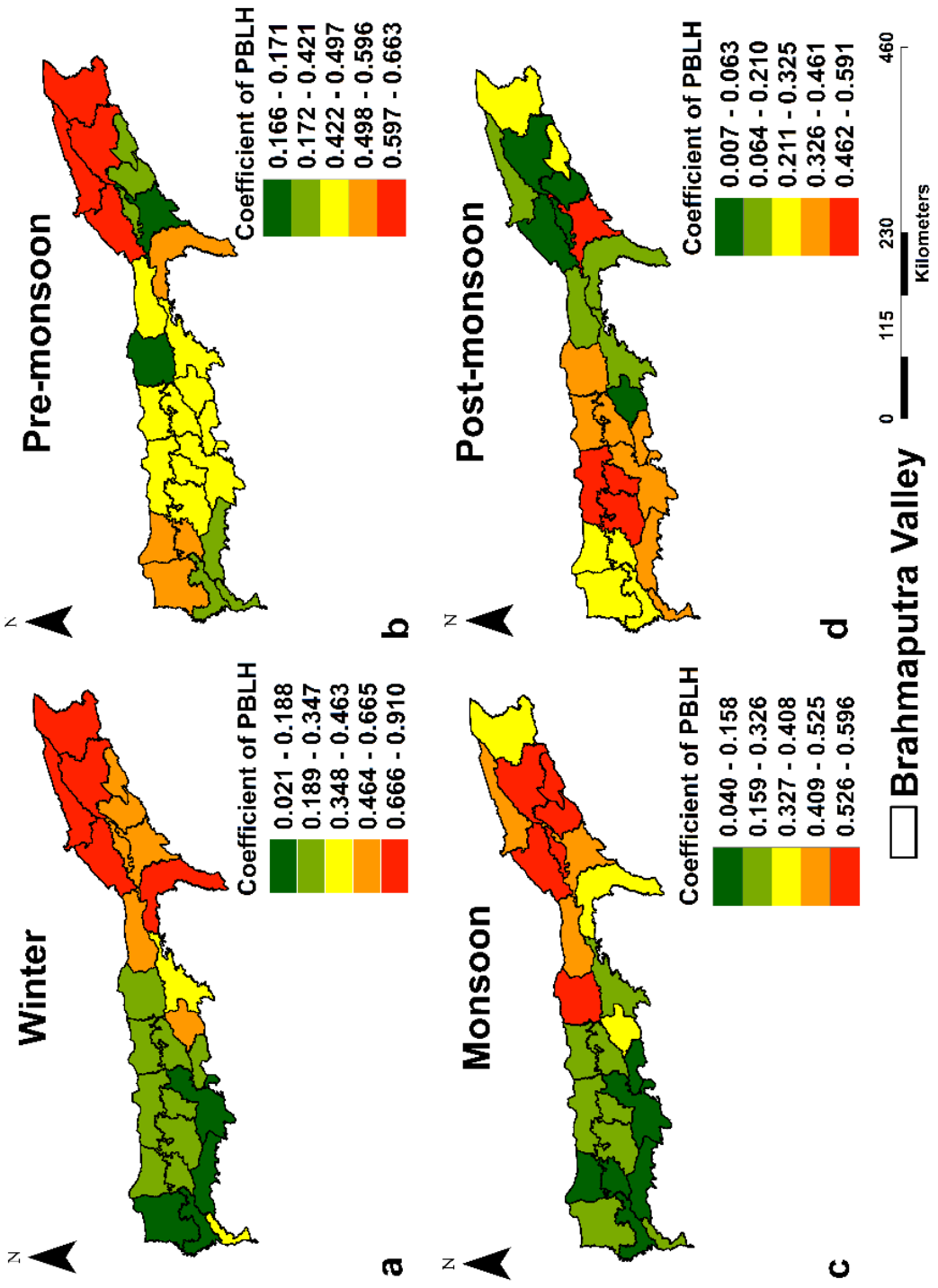

Figure 3.9 Spatial distribution of Pearson's correlation coefficient between PBLH and PM2.5 µg/m^3 over Brahmaputra valley, 2016-2020, in (a) winter, (b) pre-monsoon, (c) monsoon and (d) post-monsoon.

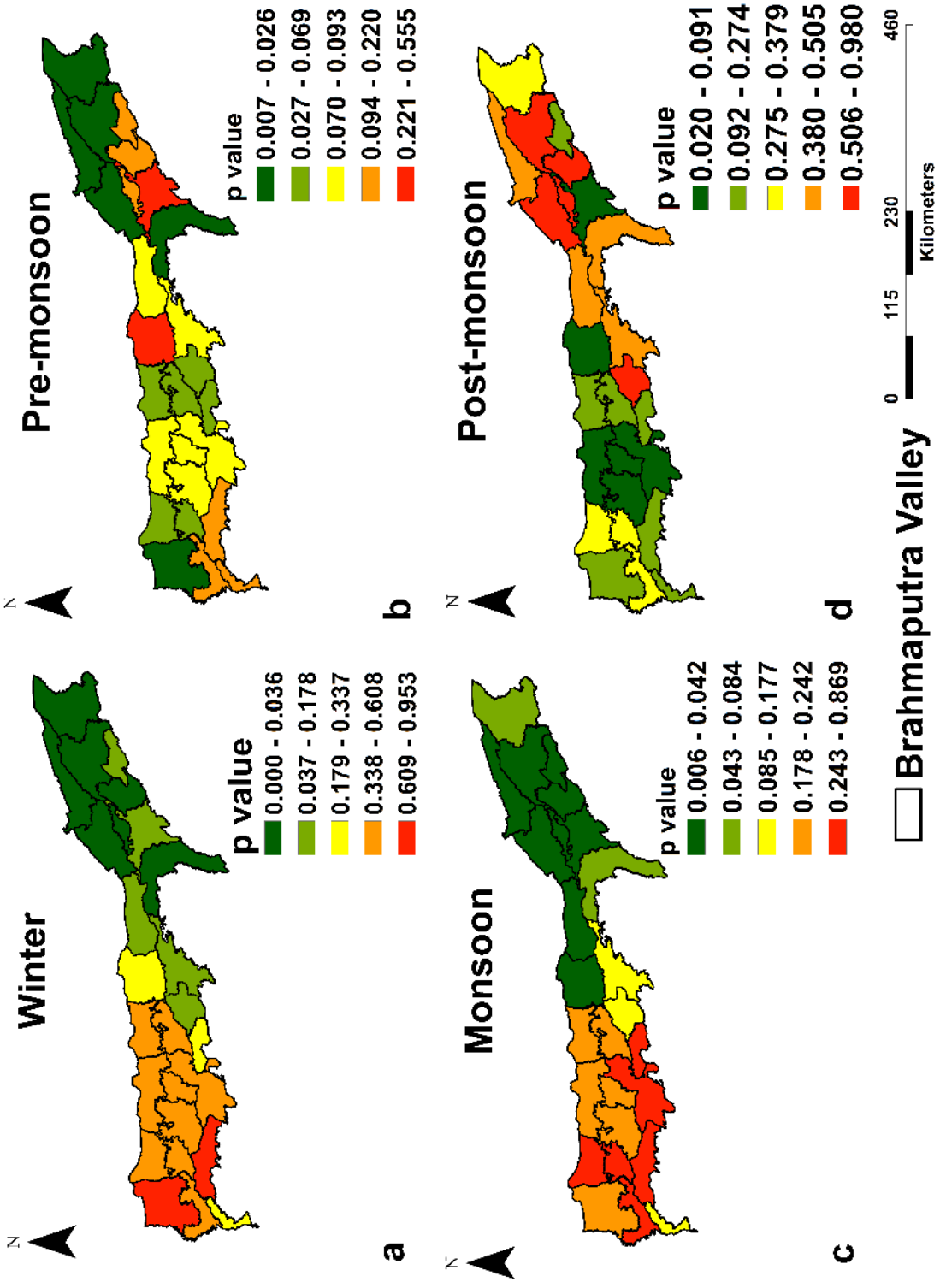

Figure 3.10 Spatial distribution of p-values of the correlation coefficient between PBLH and PM2.5 µg/m^3 over Brahmaputra valley, 2016-2020, in (a) winter, (b) pre-monsoon, (c) monsoon, and (d) post-monsoon. p-values ≤0.05 indicate significance at the 0.05 level (2-tailed).

3.5 CONCLUSION

Diurnal variation of PBLH and PM2.5 was pronounced. Deeper PBLH was observed during the day-time. The diurnal variability of PM2.5 surface concentration was in synergy with the diurnal variation of PBLH over BV. During day-time deeper PBLH (up to 2100 m in pre-monsoon) contributed to low PM2.5 surface concentration due to convective turbulent mixing developed over the valley. While at night-time nocturnal radiative cooling of the surface caused shallow PBLH confining aerosol vertical mixing thus increasing surface concentration of PM2.5. The pronounced diurnal variability of PBLH over BV is possibly driven by terrain-induced flow modification due to the heating and cooling of hill slopes over BV, a common phenomenon over complex terrain. Diurnal variation in PM2.5 surface concentration showed strong synergy with the diurnal variation of PBLH over the BV. PBLH was observed to be much higher in the day-time than at night-time, and PM2.5 concentration was lower during the day-time than night-time.

A clear synergy existed between PBLH and PM2.5 surface concentration in all the seasons over the valley. Shallow to deep PBLH was observed from west to east BV, which could be due to the localised topographic influence on the turbulence process. The surface heterogeneity of the eastern part is more as compared to other parts. Dense vegetation cover, small hill ranges and vast floodplains prevailing over the eastern zone could favour the development of strong mechanical and convective turbulence (eddy motion). The findings reveal that the PBLH structure varied with the underlying surface roughness and the turbulence generated across the valley, which in consequence affects the surface concentration of PM2.5 and AOD 550 nm.

PBLH-PM2.5 relationship showed remarkable spatial variation over the valley. The easternmost parts of the valley had consistently represented a strong positive PBLH-PM2.5 relationship for three consecutive seasons- winter, pre-monsoon and monsoon; while the central and western parts were noted with weak to moderate positive relation. The findings of this study are crucial for understanding the aerosols-PBLH feedback mechanism, and could be effectively used to determine the regulating factors of air quality at the regional level.

This study also explored different data sources for PBLH- an important step for a region otherwise known for data scarcity. MERRA-2 PBLH outperformed ERA5 ECMWF BLH

when compared with radiosonde PBLH estimates for the Dibrugarh station, for 2016-2019. Since MERRA-2 PBLH is retrieved based on the total eddy diffusion coefficient of heat (K_h) that captures the vertical turbulent diffusivity, it represents the radiosonde PBLH estimates. This study also shows that the vertical gradient of WS is an effective method for estimating PBLH for early morning hours over a complex terrain.

3.6 REFERENCE

[1] Stull, R. B. *An introduction to boundary layer meteorology*. Springer Science & Business Media, 1988.

[2] Garratt, J. R. The atmospheric boundary layer. *Earth-Science Reviews*, 37(1-2):89-134, 1994.

[3] Medeiros, B., Hall, A., and Stevens, B. What controls the mean depth of the PBL? *Journal of Climate*, 18(16):3157-3172, 2005.

[4] Seidel, D. J., Zhang, Y., Beljaars, A., Golaz, J. C., Jacobson, A. R., and Medeiros, B. Climatology of the planetary boundary layer over the continental United States and Europe. *Journal of Geophysical Research: Atmospheres*, 117(D17), 2012.

[5] Oke, T. R. *Boundary layer climates.* Routledge, 2nd edition, 2002.

[6] Finnigan, J. J. Boundary Layer (Atmospheric) and Air Pollution Complex terrain. In *Encyclopedia of Atmospheric Sciences*, 2nd Edition, Volume 1, pages 242-249. Elsevier, 2015.

[7] De Wekker, S. F. J. and Kossmann, M. Convective Boundary Layer Heights Over Mountainous Terrain—A Review of Concepts. *Frontier in Earth Science*, 3:77, 2015.

[8] Miao, Y., Liu, S., Zheng, Y., Wang, S., Chen, B., Zheng, H., and Zhao, J. Numerical study of the effects of local atmospheric circulations on a pollution event over Beijing–Tianjin–Hebei, China. *Journal of Environmental Sciences*, 30:9-20, 2015.

[9] Li, Z., Guo, J., Ding, A., Liao, H., Liu, J., Sun, Y., Wang, T., Xue, H., Zhang, H., and Zhu, B. Aerosol and boundary-layer interactions and impact on air quality. *National Science Review*, 4(6):810-833, 2017.

[10] Petaja, T., Jarvi, L., Kerminen, V. M., Ding, A. J., Sun, J. N., Nie, W., Kujansuu, J., Virkkula, A., Yang, X., Fu, C. B., and Zilitinkevich, S. Enhanced air pollution via aerosol-boundary layer feedback in China. *Scientific Reports*, 6(1):1-6, 2016.

[11] Arya, S. P. *Air pollution meteorology and dispersion.* New York: Oxford University Press, 1999.

[12] Breuer, H., Acs, F., Laza, B., Horvath, A., Matyasovszky, I., and Rajkai, K. Sensitivity of MM5-simulated planetary boundary layer height to soil dataset: comparison of soil and atmospheric effects. *Theoretical and Applied Climatology*, 109(3):577-590, 2012.

[13] Feingold, G., Jiang, H., and Harrington, J. Y. On smoke suppression of clouds in Amazonia. *Geophysical Research Letters*, 32(2), 2005.

[14] Su, T., Li, Z., and Kahn, R. Relationships between the planetary boundary layer height and surface pollutants derived from lidar observations over China: regional pattern and influencing factors. *Atmospheric Chemistry and Physics*, 18(21):15921-15935, 2018.

[15] Liu, S. and Liang, X. Z. Observed diurnal cycle climatology of planetary boundary layer height. *Journal of Climate*, 23(21):5790-5809, 2010.

[16] Miao, Y., Li, J., Miao, S., Che, H., Wang, Y., Zhang, X., Zhu, R., and Liu, S. Interaction between planetary boundary layer and $PM_{2.5}$ pollution in megacities in China: a review. *Current Pollution Reports*, 5(4):261-271, 2019.

[17] Tiwari, S., Dumka, U. C., Gautam, A. S., Kaskaoutis, D. G., Srivastava, A. K., Bisht, D. S., Chakrabarty, R. K., Sumlin, B. J., and Solmon, F. Assessment of PM2.5 and PM10 over Guwahati in Brahmaputra River Valley: Temporal evolution, source apportionment and meteorological dependence. *Atmospheric Pollution Research*, 8(1):13-28, 2017.

[18] TERI. *Risk Assessment and Review of Prevailing Laws, Standards, Policies and Programmes to Climate Proof Cities*. Synthesis Report for Guwahati, 2013.

[19] Gogoi, M. M., Krishna Moorthy, K., Babu, S. S., and Bhuyan, P. K. Climatology of columnar aerosol properties and the influence of synoptic conditions: First-time results from the North-eastern region of India. *Journal of Geophysical Research: Atmospheres*, 114(D8), 2009.

[20] Pathak, B., Kalita, G., Bhuyan, K., Bhuyan, P. K., and Moorthy, K. K. Aerosol temporal characteristics and its impact on shortwave radiative forcing at a location in the northeast of India. *Journal of Geophysical Research: Atmospheres*, 115(D19), 2010.

[21] Pathak, B., Borgohain, A., Bhuyan, P. K., Kundu, S. S., Sudhakar, S., Gogoi, M. M., and Takemura, T. Spatial heterogeneity in near surface aerosol characteristics across the Brahmaputra valley. *Journal of Earth System Science*, 123(4):651-663, 2014.

[22] Li, Q., Jiang, J. H., Wu, D. L., Read, W. G., Livesey, N. J., Waters, J. W., Zhang, Y., Wang, B., Filipiak, M. J., Davis, C. P., and Turquety, S. Convective outflow of South Asian pollution: A global CTM simulation compared with EOS MLS observations. *Geophysical Research Letters*, 32(14), 2005.

[23] Gogoi, M. M., Pathak, B., Moorthy, K. K., Bhuyan, P. K., Babu, S. S., Bhuyan, K., and Kalita, G. Multi-year investigations of near surface and columnar aerosols over Dibrugarh, North-eastern location of India: Heterogeneity in source impacts. *Atmospheric Environment*, 45(9):1714-1724, 2011.

[24] Chakrabarty, R. K., Garro, M. A., Wilcox, E. M., and Moosmuller, H. Strong radiative heating due to wintertime black carbon aerosols in the Brahmaputra River Valley. *Geophysical Research Letters*, 39(9), 2012.

[25] Barman, N. and Gokhale, S. Urban black carbon-source apportionment, emissions and long-range transport over the Brahmaputra River Valley. *Science of the Total Environment*, 693:133577, 2019.

[26] Murthy, B. S., Latha, R., Srinivas, R., and Beig, G. Particulate Matter and Black Carbon in the Brahmaputra valley of Northeast India: Observations and Model Simulation. *Pure and Applied Geophysics*, 177(12):5881-5893, 2020.

[27] Ding, F., Iredell, L., Theobald, M., Wei, J., and Meyer, D. PBL Height From AIRS, GPS RO, and MERRA-2 Products in NASA GES DISC and Their 10-Year Seasonal Mean Intercomparison. *Earth and Space Science*, 8(9), 2021.

[28] Blackadar, A. K. Boundary layer wind maxima and their significance for the growth of nocturnal inversions. *Bulletin of the American Meteorological Society*, 38(5):283-290, 1957.

[29] Arya, S. P. S. Parameterizing the height of the stable atmospheric boundary layer. *Journal of Applied Meteorology and Climatology*, 20(10):1192-1202, 1981.

[30] Hand, J. L., Copeland, S. A., McDade, C. E., Day, D. E., Moore, J. C. T., Dillner, A. M., Pitchford, M. L., Indresand, H., Schichtel, B. A., Malm, W. C., and Watson, J. G. Spatial and seasonal patterns and temporal variability of haze and its constituents in the United States, IMPROVE Report V. *Cooperative Institute for Research in the Atmosphere, Fort Collins*, 2011.

[31] von Engeln, A. and Teixeira, J. A planetary boundary layer height climatology derived from ECMWF reanalysis data. *Journal of Climate*, 26(17):6575-6590, 2013.

[32] Pathak, H. S., Satheesh, S. K., Nanjundiah, R. S., Moorthy, K. K., Lakshmivarahan, S., and Babu, S. N. S. Assessment of regional aerosol radiative effects under the SWAAMI campaign–Part 1: Quality-enhanced estimation of columnar aerosol extinction and absorption over the Indian subcontinent. *Atmospheric Chemistry and Physics*, 19(18):11865-11886, 2019.

[33] Ramana, M. V., Krishnan, P., Muraleedharan Nair, S., and Kunhikrishnan, P. K. Thermodynamic structure of the Atmospheric Boundary Layer over the Arabian Sea and the Indian Ocean during pre-INDOEX and INDOEX-FFP campaigns. In *Annales Geophysicae*, 22(8):2679-2691, 2004.

[34] Ramachandran, S. and Rajesh, T. A. Black carbon aerosol mass concentrations over Ahmedabad, an urban location in western India: comparison with urban sites in Asia, Europe, Canada, and the United States. *Journal of Geophysical Research: Atmospheres*, 112(D6), 2007.

[35] Srivastava, A. K., Singh, S., Pant, P., and Dumka, U. C. Characteristics of black carbon over Delhi and Manora Peak- a comparative study. *Atmospheric Science Letters*, 13(3):223-230, 2012.